

EFFECTS OF HIGH TEMPERATURES AND PRESSURES ON CATHODE AND ANODE INTERFACES IN HALL-HEROULT ELECTROLYTIC CELLS

Lyne St-Georges¹, László István Kiss¹, Mathieu Rouleau¹, Jens Bouchard¹, Daniel Marceau¹
¹ Université du Québec à Chicoutimi; 555 boul. de l'Université; Chicoutimi, Québec, G7H 2B1, Canada

Keywords: cathode interfaces, anode interfaces, electrolytic cell

Abstract

This paper deals with the physical modifications occurring at high temperatures and pressures at the interfaces found in the anode and cathode of a Hall-Heroult electrolytic cell. The anode and the cathode are fabricated from carbon blocks, with steel bars inserted and sealed with cast iron. Consequently, two different types of interface are found in the anode and the cathode assembly: cast-iron with steel and cast-iron with carbon. For the investigation presented here, an experimental setup was built to heat and load anode and cathode samples. Specific attention was put on the sample preparation, to reproduce real cathode/anode sealing conditions. During the heating and the loading of the samples, fluctuations of electrical and thermal contact resistances were observed and related to physical transformation at the interfaces. These transformations could potentially explain the non-homogeneities of voltage and current distribution occurring in a Hall-Heroult electrolytic cell.

Introduction

The anodes and the cathodes of a Hall-Heroult electrolytic cell are composed of carbon blocks in which steel rods or bars are inserted. To provide a good electrical and thermal contact and to give good mechanical strength to the steel and carbon assembly, liquid iron is cast between the steel rods/bars and the carbon block to seal the anode or the cathode. The quality of the contact between the components used in the anode and cathode is of primary importance because a great amount of energy is transmitted through these interfaces to the electrolytic process. During the aluminum electrolysis, a bad contact between the cast-iron and the carbon block or between the steel and the cast-iron can modify the current and the heat distribution in the electrodes and decrease the effectiveness of the electrolytic cell.

For 30 years, many efforts have been made to quantify experimentally or *in-situ* the voltage and the temperature drops at the cast iron / carbon interface on the cathodes and the anodes of the electrolytic cells [1-6]. These voltage and thermal drops are expressed in terms of electrical and thermal contact resistance respectively.

The contact resistances normally decrease with the applied pressure. This phenomenon can be explained by the augmentation of the real area of contact (or the increase of the number of contact points) with the pressure. This increase of the contact surface decreases the throttling of the current lines at the interface, responsible for the contact resistance, and consequently decreases the contact resistance. Furthermore, based on the literature review, the contact resistances are also expected to be reduced by an increase of the temperature. As the temperature increases, the mechanical strength of the material decreases, asperities begin to collapse and the real contact surface increases. This augmentation

of the contact surface reduces the contact resistance. Among all the investigations presented in the literature on the subject, some authors have reported higher values than those predicted by theoretical models and irregularities at high temperature [5-6].

In this paper, the effect of high temperatures and pressures at the anode and cathode interfaces on the electrical and thermal contact resistances is investigated. The specific interfaces considered are those in the anode and the cathode of an electrolytic cell:

- anodic cast iron / steel stub rod;
- anodic cast iron / carbon;
- cathodic cast iron / steel of collector bar;
- cathodic cast iron / carbon.

Material properties

The anode and the cathode carbon used are different materials with specific composition and properties. The main differences between these two materials are listed in the Table 1. For the sealing of anodes and cathodes, different cast iron is also used. The main difference between the two types of iron used stands in the material composition. Both the anode and the cathode cast-iron are of the grey type.

Table 1 : Differences between anode and cathode carbon

	Anodic carbon	Cathodic carbon
Composition	Coke+Pitch	Anthracite+Pitch
Graphitization	Non-graphitized	Partially graphitized
Porosity	Relatively porous	Relatively less porous than anodic carbon
Hardness	Low	Relatively hard, function of the graphitization

Sample preparation

To produce test samples, the steel, the cast-iron and the carbon samples (both anode and cathode) were fabricated to reproduce the surface characteristics obtained in industrial anodes and cathodes. The steel samples were obtained directly from the steel supplier. Cylindrical samples with a diameter of 50.8 mm and a length of 330.2 mm were used for the experiments. The cathode and the anode carbon samples were cut respectively from an industrial cathode and anode block. Cylindrical samples with a diameter of 50.8 mm and a length of 330.2 mm were extracted. The surfaces of the samples were not modified from the carbon block to conserve their original characteristics.

The carbon and the steel samples were placed separately in hollow graphite tubes (508 mm long with an internal diameter of 50.8 mm and an outside diameter of 76.2 mm). These tubes, with either the carbon or the steel samples, were inserted into an anode carbon block to provide the same cast iron cooling rate as that

used in industrial anode sealing. The carbon block was then heated with the samples up to 100°C (the normal cell pre-heating temperature used in anode/cathode sealing). Once the temperature was reached, the melted iron was cast at the top of the carbon and the steel samples, using an industrial anode sealing procedure to form the cast-iron/carbon and cast-iron/steel pairs of samples. Once cooled, the pairs of samples were delicately extracted from the carbon block using a hydraulic press. For the fabrication of the cathode samples, based on numerical simulations, two side-by-side anode blocks were used instead of a cathode block to provide a cooling rate similar to that obtained in industrial cathode sealing.

Experimental tests

The apparatus used to heat and load the samples was designed to determine both electrical and thermal contact resistance [7]. Figure 1 shows the experimental set-up used. In the apparatus, the samples are placed vertically between two electrodes. A furnace is used to heat the pair of samples and the geometry of the electrode outside the furnace is designed to act as a heat sink to create a heat flux in the samples through their interface. The samples are connected into an electrical circuit by the electrodes and consequently, a voltage and a temperature gradient are created through the test section. A measurement of the electrical and thermal contact resistances at the interface is then possible.

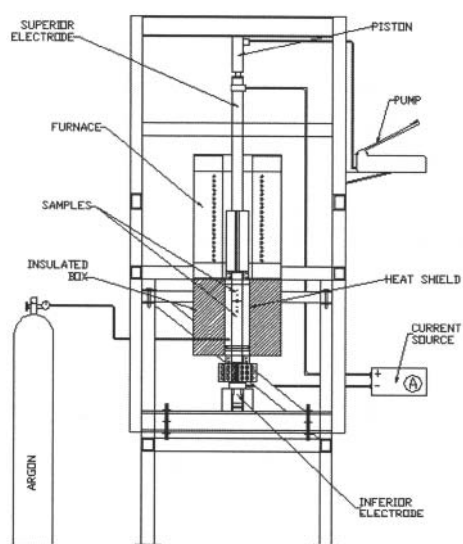


Figure 1: Apparatus used to heat and load the samples

In the apparatus presented, the samples were protected from oxidation by various means: (1) the oxygen was purged by injection of argon in the furnace cavity. A semi-hermetic sheet metal retained the argon around the sample and a pressure gage was used to maintain the argon pressure higher than the atmospheric pressure, to avoid oxygen inlet in the system; (2) an anti-oxidation coating was applied on the samples. This anti-oxidant is very stable at high temperature and non-conductive thermally and electrically; (3) a small carbon piece was placed in the furnace, between the samples and the thermal shell and acts as a sacrificial sample to rapidly consume the oxygen before a reaction takes place with the samples.

For the experimental determination of the contact resistances, the samples were then heated, using the experimental setup, up to 1000 °C, using steps of 150°C (except for the last step, from 800°C to 1000°C). For each step of temperature, steady-state contact resistance was measured with applied pressures between 0.5 MPa and 2.5 MPa. These temperatures and pressures were used to reproduce the conditions found in an electrolytic cell. For each step of temperature, the conditions were maintained for 24 hours to reach a thermal steady-state condition. Each level of pressure was then applied for 2 hours (10 hours total) after which the steady-state measurements were taken. After the heat and pressure cycles experiment, electron and optical microscopes were used for microstructure and macroscopic observations.

Results and discussion

Figure 2 shows the typical variation of the contact resistance obtained. Globally and as expected, the resistance decreases as the temperature increases. However, at about 550 °C, an augmentation of the resistance is observed. This behavior occurs in all the samples tested, but is more visible in the results obtained for the electrical contact resistances.

For the material tested, various metallurgical and mechanical transformations may occur during the experiment process:

- desorption of oxygen by the carbon;
- carbon combustion;
- hardening of the cast iron surface (during the iron casting);
- annealing;
- chemical reactions in the cast iron;
- cast iron creep;
- welding between the steel and the cast-iron;

These transformations could explain the fluctuations of the resistance observed and their effects are discussed in the following sections.

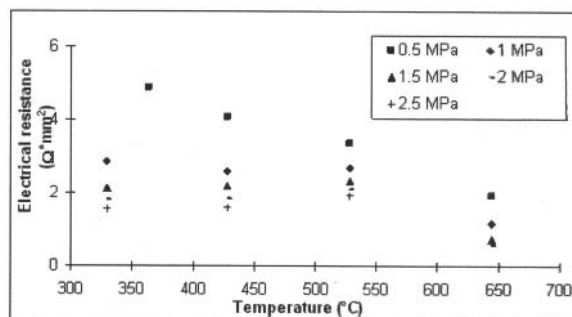


Figure 2: Variation of the electrical contact resistance between cathodic cast iron and carbon

Oxygen desorption and carbon combustion

The observations made on the carbon samples have shown that the surface of the carbon samples was consumed during the test procedure. Considering the porosity of the carbon sample and the presence of several barriers to the oxygen inlet in the experimental device used, it appears that the oxygen does not come from outside the system but from the sample themselves.

The oxygen adsorption by the carbon at low and high temperature is a known phenomenon. The carbon being relatively porous, a non negligible quantity of oxygen is adsorbed by the carbon surface before the sample fabrication. When heated at elevated temperatures, the oxygen reacts with the carbon. The carbon combustion has been frequently observed at temperature about 500-600°C. This range of temperature also coincides with the temperature of carbon desorption (550°C, [8]).

Heat treatment of cast iron

The microstructure of the iron is highly dependent on its thermal history. To evaluate the impact of the heating procedure on the microstructure of the iron used, micro-hardness measurements were made at several points along the depth of a non-heated (as fabricated) cast-iron sample and compared to a cast-iron sample after a normal heating procedure used during the experiments. For the hardness measurements, the samples were cut along their longitudinal axis and the measurements were made from the surface (depth ≈ 0) to their opposite ends. Figure 3 shows the effect of the heating procedure on the micro-hardness of the cast iron, along the depth axis. The micro-hardness is higher for the as-cast sample than for the heated samples. Moreover, in contrast to the heated sample, the micro-hardness is significantly higher near the contact zone (depth ≈ 0) for the as-cast sample. For the heated sample, the hardness is nearly constant over the depth.

The surface hardening observed for the as-cast sample is produced by the fabrication procedure used: the liquid iron, initially heated at a temperature of 1400°C, is poured on a carbon block at 100°C. The instantaneous contact between the liquid iron and the carbon block causes a rapid cooling of the iron surface and produces the surface hardening.

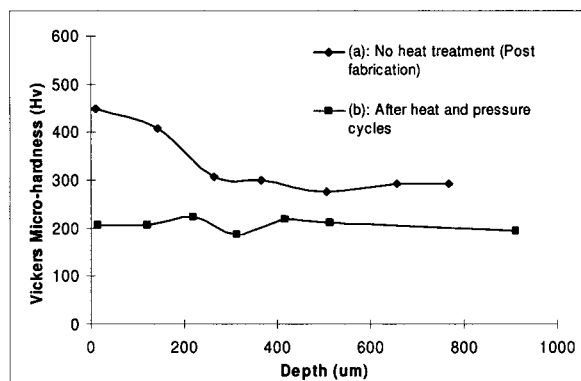


Figure 3: Vickers micro-hardness of (a) a non heat-treated and (b) a heat treated cast iron

On the other hand, when heated at elevated temperature, the grey cast iron is subject to the following heat treatment [9]: (1) annealing (which eliminates the residual stresses generated by heterogeneous cooling); (2) ferritic annealing (which transforms the perlite into graphite and ferrite, resulting in a decreased hardness). These transformations also occur in the iron samples during the experiments. They are responsible for the hardness reduction and homogenization of the heated samples.

To analyze the effect of the heating procedure on the iron, the microstructures of the samples used for the micro-hardness

measurement were analyzed with an scanning electron microscope (SEM) equipped with an Energy Dispersive Spectrometer (EDS). The microstructures of the as-cast sample (non-heated) and of the heated sample after an experiment are presented in Figure 4. The as cast samples exhibit graphite plates near the surface. The graphite plates are generally produced by a very fast cooling rate [10] and are representative of the anode/cathode sealing process, where a fast solidification is obtained.

For the heated sample, the heating during the experiment increases the size of the graphite plates. The large graphite plates, which are more numerous in the heated sample than in the as-cast sample, reduce the cast iron hardness and its electrical resistivity [11].

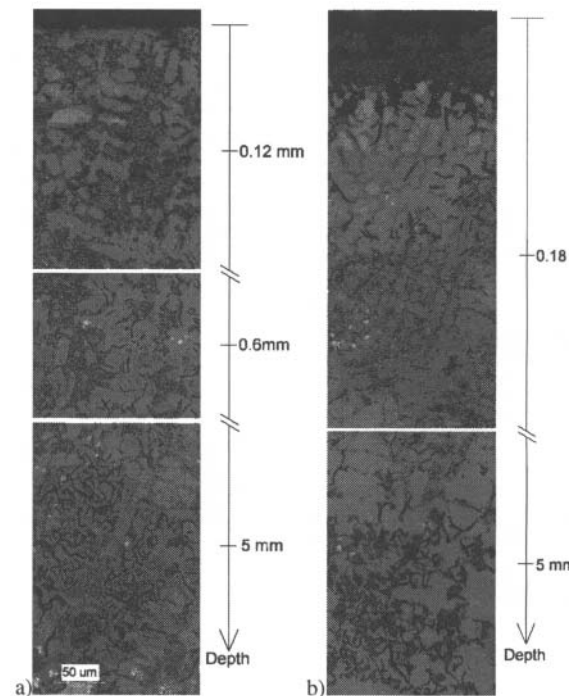


Figure 4: 500X Micrographies of grey cast-iron phases: a) as cast sample b) heat treated sample

Cast iron modifications during the experiments

After the heating procedure used to determine the contact resistance at elevated temperature, an extremely friable, thin, grey-blue layer, not seen before, was observed between the heat treated cast-iron and the carbon samples (both anode and cathode). This layer, observed in the test samples, is related to the relatively long exposure to high temperatures. For similar environmental conditions, three specific phenomena are normally observed in iron: surface decarburization, surface oxidation and surface oxidation with the presence of silicon.

To determine the nature of the transformations observed, the surface of the cast iron was analyzed with an electron microscope. Pictures of the iron surface, after heating, are presented in Figure 5 for various magnifications (a to c), and compared with a cast iron sample, not heated (d). For the heated cast iron surface, two

dark gray layers are observed. To determine the chemical composition of these layers, a Wavelength Dispersion Spectrometer (WDS) was used. The composition maps obtained are presented in Figure 6.

The first layer observed is rich in oxygen and iron and the second layer is mainly composed of oxygen, silicon and iron. The composition of the first layer is representative of the presence of an iron oxide (such as FeO). The FeO, also called Wustite, is a p-type semi-conductor and is formed from 570°C [12], which is about the temperature of sudden jump of contact resistance observed in Figure 2. For the second layer, a silicon dioxide (silica) containing iron is suspected (SiO_2 + Iron oxide for example). In the iron, the silicon can be oxidized to form silica [13]. The oxygen needed for these chemical reactions may come from the carbon desorption, as mentioned before.

The decarburization at the surface of the cast iron, clearly visible in Figure 5, is also observable in Figure 4 (at a depth ≤ 0.18 mm). This decarburization seems to be due to chemical reactions between the carbon contained in the cast iron and the oxygen adsorbed by the carbon sample in contact with the iron, to form gaseous CO and CO_2 . This phenomenon of cast iron decarburization is well known and reported in the literature [11, 13]. In addition to the carbon impoverishment of the cast iron produced by the decarburization, other oxidation or reduction mechanisms may occur: (1) oxidation of the iron contained in the cast iron; (2) removal of the exposed graphite by oxidation to carbon monoxide [83].

The friability of the grey blue thin layer observed after heating can be explained by the oxidation of the iron. It is known that over 700°C, the carbon monoxide and dioxide removal can create cracks and swelling in the iron. In the lamellate graphite, the graphite plates facilitate the oxygen penetration inside the cast iron and oxidized layers can then be produced inside the iron. These metallic oxide layers have a volume greater than the volume previously occupied by the metal, and may produce cracks and swelling of the iron, expose new surfaces to the oxygen and accelerate the oxidation process [11]. The decarburization as well as the oxidation of the iron has an important effect on the contact resistance since the cast iron conductivity is greatly dependent on the carbon content.

The decarburization of the cast iron can be a priori difficult to accept, considering the presence of the carbon in contact with the cast iron in the pair sample. The diffusion or the migration of an element follows the direction opposed to the gradient of concentration of the element itself and, consequently, a carbon enrichment of the iron instead of an impoverishment would be expected.

To explain this behavior and to visualize the real surface of contact between the carbon and the iron in the samples produced, a sample was cut, epoxy mounted and polished for microscopic observations. In the sample preparation, a mechanical pressure of 1 MPa was applied during the epoxy solidification to reproduce test conditions. A typical micrograph of the carbon / cast iron interface obtained under this condition of preparation is shown in Figure 7.

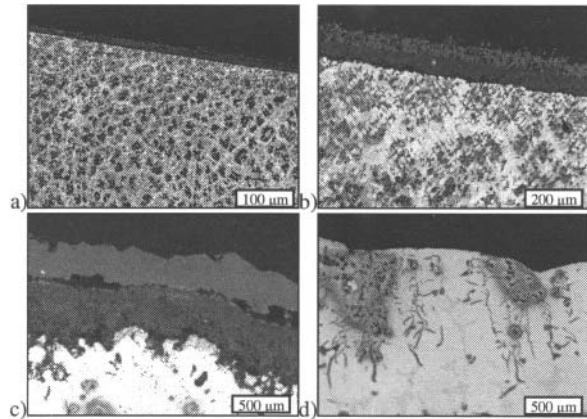


Figure 5: Cast iron surface, heated sample at (a) 25X, (b) 100X, (c) 500X and non-heated sample at (d) 500 X

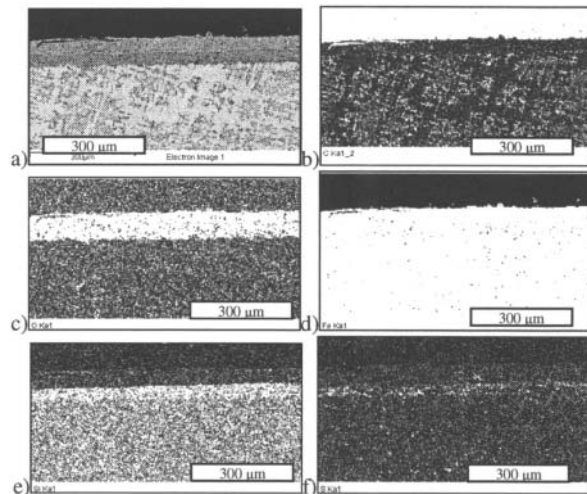


Figure 6: Chemical analysis of cast iron surface. Clear pixels represent high concentration of (b) carbon; (c) oxygen; (d) iron; (e) silicon; (f) sulphur; (a) is a 200X optical micrograph

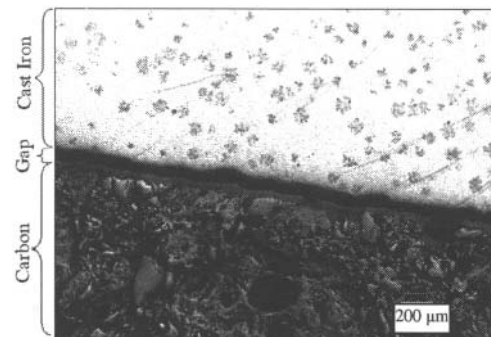


Figure 7: Evidence of gap at the cast-iron/carbon interface under a mechanical pressure of 1 MPa

A gap is observed between the carbon and the cast iron. In fact, a good contact is obtained only at a limited number of points. The gap between the cast iron and the carbon samples (approximately equal to 75 μm) is greater than the gases mean free path, even at elevated temperature. Consequently, CO and CO_2 displacements

are possible. This gap between the two materials is a potential obstacle to the diffusion and probably stops the diffusion of the carbon towards the cast iron. However, this spacing is large enough to allow oxygen, CO and CO₂ to circulate at the interface and to escape.

During the sample fabrication and the anode / cathode sealing, the liquid iron is poured directly on the carbon. The presence of the gap observed may have different sources (gas trapping, withdrawal...) but can be partially explained by the thermal contraction of the cast iron during its cooling. In reality, cast iron shrinkage is about 1%, which is sufficient to produce the gap illustrated in Figure 7.

Cast iron creep

During the heating and the loading cycles, under steady-state conditions of loading, it was observed that, for a constant displacement imposed, the pressure applied on the samples goes down with time, especially at elevated temperatures. This phenomenon could be explained by the creep in compression of the cast iron. It is known that the creep of the cast iron can become important when the material is heated at elevated temperatures [11]. The cast iron creep could increase the real surface of contact between the surfaces and thus reduce the contact resistance.

Steel and cast-iron welding

For the cast-iron/steel samples (anode and cathode pairs), an unexpected welding phenomenon was observed: welded spots with surfaces of about 150 mm² were observed between the cast-iron and the steel samples. Figure 8 shows a typical weld broken for observation purposes. On each sample, only one of these spots was observed. This welded spot could be related to a local melting of the steel sample during the sample fabrication and is typically located where the liquid iron falls directly on the steel, i.e. where the heat is sufficient to melt locally the steel sample.

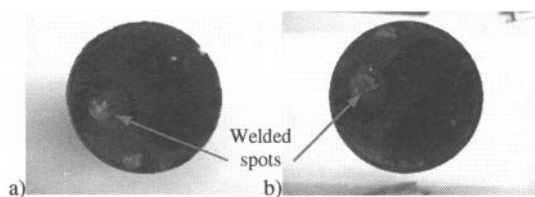


Figure 8: Broken welded spots between (a) cast-iron and (b) steel

The metallurgical links created by the welding between the steel and the cast-iron have an extremely important impact on the current and heat transfer. For the cast-iron/steel samples, the assumption of uniform voltage distribution fails.

This first observation gives more insight on the cast-iron/steel interfaces but needs to be validated for real electrolytic cells. The procedure used to produce the cast-iron/sample is representative of the one used for the anode/cathode sealing and should provide at least a similar cooling rate. However, for large samples or during the sealing of an industrial cathode or anode, only a limited number of welding points are expected, where the heat provided by the liquid iron is large enough to melt the steel. To confirm this expectation and to validate the presence of these welded spots in industrial electrolytic cells, further work is needed.

Conclusions

During the heating of cathodes and anodes, several physical transformations may occur at the cast iron/steel and cast iron/carbon interfaces. The decarburization and the oxidation of the carbon/iron interface, the welding of the iron/steel interface and the material creep are the only potential transformations noticed in this investigation. More complex or combined transformations may occur in industrial anode/cathode interfaces and interface transformations being susceptible to variation with time, the contact resistances should also vary with time. These transformations have important effects on the contact resistances and could explain the electrical and thermal distributions heterogeneity observed in the electrolytic cells.

Acknowledgements

This work is part of the research program of CRDA (Centre de Recherche et de Développement Arvida) of Rio Tinto Alcan and was also supported by the CURAL (Centre Universitaire de Recherche sur l'Aluminium), part of the Université du Québec à Chicoutimi.

References

- [1] R.W. Peterson "Temperature and voltage measurements in hall cell anodes", *Light Metals*, Vol 1, 1976, p. 365.
- [2] D.G. Brooks, V.L. Bullough, "Factor in the design of reduction cell anodes", *Light Metals* 1984, p. 961.
- [3] P.J. Rheday, L. Castonguay, "Effects of carbaceous rodding mix formation on steel-carbon contact resistance", *Light Metals* 1985, p. 1089.
- [4] M. Sorlie, H. Gran, "Cathode collector bar to carbon contact resistance", *Light Metals* 1992, p. 779.
- [5] F. Hiltmann, H. A. Øye, "Influence of temperature and contact pressure between cast iron and cathode carbon on contact resistance", *Light Metals* 1996, p. 277.
- [6] L.I. Kiss, M. Rouleau, L. St-Georges, "Determination of the thermal and electrical contact resistances at elevated temperatures", *Proceeding of the twenty-eight international thermal conductivity conference*, 2006, p. 224.
- [7] St-Georges, L., Kiss, K.I., Rouleau, K., « Evaluation of contact resistance in electrodes of Hall-Heroult process», *Light Metals* 2009, p. 1103.
- [8] Le groupe français d'étude des carbones, « Les carbones », Tome 2, Masson et Cie, 1965.
- [9] J-M. Dorlot, J-P. Baillon, J. Masounave, «Des matériaux», 2^{ième} édition, Édition de l'école Polytechnique de Montréal, 1986.
- [10] F. Barralis, G. Maider, «Précis de Métallurgie», AFNOR, p. 58.

[11] Centre d'information des fontes moulées, « Manuel des fontes moulées », Éditions Techniques des industries de la fonte, 1963, p. 705.

[7] A.S. Khanna, «Introduction to high temperature oxidation and corrosion », ASM International, 2002, p. 82.

[83] W.F. Charles, «Gray and Ductile iron casting handbook», Editions Cleveland Ohio, 1971, p. 679.

[94] S.C. Saxena, R.K.Joshi «Thermal accommodation and adsorption coefficients of gases», Hemisphere publishing corporation, United-States, 1989.